On the Outage Probability of Millimeter Wave Links with Quasi-deterministic Propagation

Amr A. AbdelNabi
IMDEA Networks Institute
University Carlos III of Madrid
amr.abdelnabi@imdea.org

Vincenzo Mancuso
IMDEA Networks Institute
vincenzo.mancuso@imdea.org

Marco Ajmone Marsan
Politecnico di Torino
IMDEA Networks Institute
marco.ajmone@polito.it

ABSTRACT

Millimeter waves are emerging as a key technology for future wireless communication systems and networks. The low transmission power allowed by regulation requires high gain steerable antenna arrays to generate directional links that can support high data rates. However, link directionality implies high sensitivity to obstructions, that can cause link outage. This paper presents a new simple analytical model based on stochastic geometry for the estimation of the outage probability of millimeter wave indoor and outdoor connections, accounting for the presence of obstructions. The accuracy of the model is proved by comparison against simulation results in a number of cases.

CCS CONCEPTS

• **Networks** → **Network performance modeling**; **Network performance analysis**; *Wireless access networks.*

KEYWORDS

Millimeter Wave, Obstructions, Outage, Analytical model

ACM Reference Format:
Amr A. AbdelNabi, Vincenzo Mancuso, and Marco Ajmone Marsan. 2019. On the Outage Probability of Millimeter Wave Links with Quasi-deterministic Propagation. In *3rd ACM Workshop on Millimeter-Wave Networks and Sensing Systems (mmNets) 2019, October 25, 2019, Los Cabos, Mexico.* ACM, New York, NY, USA, 6 pages. https://doi.org/10.1145/3349624.3356762

1 INTRODUCTION

According to the latest version of the Cisco Visual Networking Index [5], "mobile data traffic will increase seven fold between 2017 and 2022", and "traffic from wireless and mobile devices will account for 71% of total IP traffic by 2022" reaching over 200 EB per month. This growth is congesting the 2.4 GHz and 5 GHz bands that are today used for wireless communications, and more generally is making the spectrum available for data communications in the range below 6 GHz insufficient. Thus, exploiting higher frequency bands, such as 28, 60, and 73 GHz, will soon become necessary to satisfy the hunger for wireless data transfer. This makes the millimeter wave (mmwave) technology a must for the networks of the coming years [2]. Using mmwaves in commercial systems is technologically challenging due to the high attenuation suffered under non-line-of-sight (non-LoS) conditions. As pointed out in [2], outage occurs because of four main reasons. First, penetration losses are very severe with commonly used materials. Second, mmwaves tend to bend around obstructions instead of being diffracted. Third, the narrow link beams used to ensure the necessary directionality weaken the ability to avoid obstructions. Fourth, the low transmission power used for mmwaves does not leave much signal to noise ratio (SNR) margin to avoid outage.

Incorporating models of outage into the analytical framework for mmwave system design is important, since outage significantly impacts design choices. Outage is usually modeled by considering self-body outage effects [4] and shadowing effects, whose impact can be represented by means of a lognormal random variable (r.v.). In [10], ray tracing was used to model outage in a deterministic environment. In [6], a random Boolean model was proposed to model outage in a mmwave cellular system; this model was further specified for rectangular [3] and circular shapes [12]. These and many of the available studies deal with outdoor environments. As regards indoor environments, most papers are based on measurements, and report up to 80 dB loss for half-meter-long obstructions and 40 dB for a 28-cm depth human body [8, 11]. The authors of [7] use queuing theory to model the duration of (self-)blockage in the presence of macro-diversity in the transmission schemes. Differently from us, no work accounts for the possibility that outage is caused by the accumulated attenuation due to more than one obstruction over any of the paths that beamsteering can select in the presence of quasi-deterministic propagation.

mmNets 2019, October 25 2019, Los Cabos, Mexico

ACM ISBN 978-1-4503-6932-9/19/10…$15.00
https://doi.org/10.1145/3349624.3356762

In this paper, we i) show how to estimate the "obstruction length", i.e., the length of the portion of a link between a transmitter and a receiver that is occupied by obstructions, accounting for LoS links as well as reflections; ii) derive a tractable expression for the outage probability, incorporating the impact of beamsteering and the effect of obstruction length through randomly placed independent obstructions; the expression holds in general for convex-shaped obstructions; iii) prove the accuracy of the proposed model by comparison against simulation in indoor and outdoor scenarios.

2 SYSTEM MODEL

We consider a wireless communication system consisting in a mmwave transmitter/receiver pair, i.e., one access point (Tx node) and one user equipment (Rx node), placed at fixed known locations, within a 2D rectangular walled environment. Mmwave signals can be reflected by walls, so that in addition to the direct (LoS) path between Tx and Rx, also paths including reflections are possible. A random number of objects with convex shape are randomly placed in the rectangular area, according to a uniform Poisson point process (PPP) with intensity λ, and their effect is to obstruct mmwave links. We assume that transmitter and receiver perfectly align thanks to beamsteering, and antennas are strongly directional, so that antenna side lobes are negligible. The beamsteering alignment is assumed to be the optimal one, which does not necessarily correspond to the direct path between Tx and Rx, which indeed might be obstructed.

We consider a quasi-deterministic channel model [13] with a direct path and a limited number (normally 4) of primary reflections, i.e., paths with a single reflection, caused by a wall. The lengths of the considered paths are the components of a vector $\mathbf{d}$, in which the first element d_1 is the LoS distance between Tx and Rx, and the other elements $d_k, k = 2, 3, 4, 5$ list the lengths of primary reflection paths in a given order.

Since beamsteering is fast and can be tuned frequently [9], we assume that it always selects the least attenuated path.

2.1 SNR computation

The Tx transmit power is denoted by P_{Tx}, while the system antenna gain after beamsteering, including both transmitter and receiver antennas, is denoted by G. The path loss L_k on link k is modeled considering free-space loss, air absorption and reflection loss. In dB units, the loss is:

$$L_k = 20 \log_{10}(4\pi f d_k / c) + M d_k + W_k, \tag{1}$$

where c is the speed of light in the air, f is the adopted mmwave frequency, M is the absorption due to the transmission medium (air) per unit length, and W_k is the wall attenuation on the selected path ($W_1 = 1$, since the direct path does not suffer reflections).

Reflected mmwaves suffer attenuation according to their polarization, frequency, refraction indexes of air and wall, and angle of incidence of the reflected wave on the wall. Specifically, the attenuation W_k is computed by means of the well-known Fresnel equations, which yield different values for each of the walls, depending on the materials considered for the walls and the specific geometry of the studied case.

The mmwave signal is further attenuated by obstructions. The length of the intersection between a link and an object is called the *per-object obstruction length*, which yields signal attenuation at rate z dB/m, depending on the obstruction material. The r.v. X_k models the *total obstruction length* over path k, i.e., the sum of obstruction lengths due to individual objects that intersect the path.

The channel coefficient for a path is denoted by h/μ_k, in which the r.v. h captures the normalized link small scale fading, and is modeled as an exponential r.v. with mean 1 (Rayleigh fading), and $1/\mu_k$ is a constant that represents the average fading depth [13]. The total average attenuation on path k, not considering the small scale fluctuations due to h, is a r.v. $a(X_k)$ that depends on X_k. So, in dB units, we have:

$$a(X_k) = L_k + 10 \log_{10} \mu_k + z X_k. \tag{2}$$

Noise is assumed to be additive Gaussian with variance σ^2, so that, by putting together all the pieces, the SNR γ_k, after steering the antennas to align with path k, is:

$$\gamma_k = \frac{P_{Tx} G\, h}{\sigma^2} 10^{\frac{-a(X_k)}{10}}. \tag{3}$$

If antennas are optimally steered at each transmission, the experienced SNR will therefore correspond to the SNR of the path that suffers the least average attenuation. This means that, once the positions of Tx, Rx and walls are known, and obstructions are placed, the beamsteering is deterministic and fixed, depending only on the path loss and the obstruction attenuation, plus an average loss due to small scale fading. Therefore, the SNR after beamsteering can be expressed as a function of the small scale fading h and of a r.v. $\Psi = \min_k \left\{10^{a(X_k)/10}\right\}$ that accounts for the fact that beamsteering selects the path that minimizes path loss $a(X_k)$:

$$\gamma = P_{Tx} G h / (\sigma^2 \Psi). \tag{4}$$

3 TOTAL OBSTRUCTION LENGTH

We discuss the computation of the total obstruction length in the case of the LoS path, but the extension to paths including reflections is straightforward, provided border effects (close to the reflection point) are neglected. Indeed, with this approximation it is possible to assimilate direct and reflected paths, by considering the latter as direct paths with lengths corresponding to the space actually traveled by the mmwave.

We assume that the total obstruction length can be computed as the sum of independent per-object obstruction

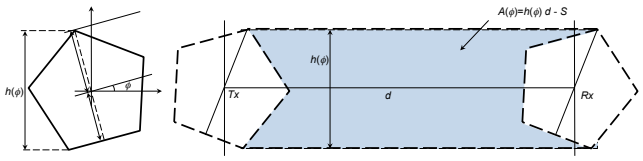

Figure 1: Area in which object centers lead to obstruction, for convex shapes

lengths. This is appropriate if the average obstruction length is much less than the link length.

Consider a rectangular portion of the plane comprising the LoS link connecting the Tx/Rx nodes. We denote by s the maximum transverse dimension of an obstruction. Furthermore, we call "center" of an obstruction the mid point on its maximal transverse dimension. Only objects with center within $s/2$ from the link can cause obstruction, hence we can consider just the rectangle with sides s and $d + s$ as the set of centers of potential obstructions. Since mmwaves suffer high attenuation, it is not interesting to study scenarios with high density of obstructions. Hence, in our model we neglect the fact that randomly placed objects might end up overlapping. We further consider that obstructions cannot overlap with Tx and Rx. As a consequence, given an object shape and a fixed rotation, there exist two regions around Tx and Rx in which no obstruction center can lay. We denote by A_1 (in the case of reflected paths we use A_k) the "sensitive area", i.e., the average area in which randomly placed centers of objects with random rotation cause obstruction. As an example, Fig. 1 shows A_1 for pentagonal obstructions.

Considering the geometry of Fig.1, the number of obstructions intersecting the LoS path (but the same is true for all paths) has Poisson distribution. This is clear for a fixed object shape and rotation, because the number of objects that fall in a deterministic area, with a uniform PPP, is Poisson. Thus, by assuming that the object shape is fixed and the rotation is uniformly picked at random in the interval $[0, 2\pi]$, the r.v. that models the number of obstructions is the weighted sum of independent Poisson r.v.'s, and it is therefore a Poisson r.v. itself. As a result, the average number of obstructions on path k is $N_k = \lambda A_k$ and the number of obstructions on path k has Poisson distribution with parameter N_k.

We use a simple approximation on the probability density function (pdf) of the per-object obstruction length. Specifically, by using a Dirac delta centered at the obstruction length average, we consider that each obstruction contributes with exactly the average per-object obstruction length l_o. This quantity only depends on the geometry of the object. In particular, for convex shapes we use the average chord length resulting from intersecting the object with a random line. The generality of this very simple model can be appreciated by considering that for any object with convex shape, the average conditional per-object obstruction length l_o is computed by means of the second Cauchy formula as

$$l_o = \pi S/P, \tag{5}$$

where S and P are respectively the area and the perimeter of the convex-shaped object. With the mentioned approximation, the total attenuation resulting from n obstructions on the k-th path, assuming the antennas are steered on that path, is simply $a(X_k|n) = L_k + 10\ \log_{10}\mu_k + z\, n\, l_o$ dB.

4 OUTAGE PROBABILITY

The outage probability is defined as the probability that the SNR γ takes a value below a given threshold γ_{th} as a function of physical transmission parameters plus obstruction effects. We next derive a generic expression for the outage probability, then we derive an approximation for the case of small obstructions, and finally show how to model the effect of different obstruction shapes.

4.1 General expression

The outage probability can be derived from (4) and corresponds to the cumulative distribution function (CDF) of the r.v. h/Ψ evaluated in $B\gamma_{\text{th}}$, where $B \triangleq \frac{\sigma^2}{P_{\text{Tx}}G}$ is a constant:

$$P_{\text{out}}(\gamma_{\text{th}}) = \Pr\left(\frac{P_{\text{Tx}}G}{\sigma^2}\frac{h}{\Psi} < \gamma_{\text{th}}\right) = \Pr\left(\frac{h}{\Psi} < B\gamma_{\text{th}}\right). \tag{6}$$

Since h is exponential, if the distribution of Ψ is known, the above formula can be conveniently rewritten as

$$P_{\text{out}}(\gamma_{\text{th}}) = 1 - \int_0^\infty e^{-B\gamma_{\text{th}}t} f_\Psi(t)dt = 1 - \mathcal{M}_\Psi(-B\gamma_{\text{th}}), \tag{7}$$

where $\mathcal{M}_\Psi(\cdot)$ is the moment generating function of Ψ.

4.2 Approximate expression

We approximate the per-object obstruction length (which is a r.v.) with its average l_o. Thus, the number of obstructions completely describes the per-path total obstruction length. Furthermore, the joint distribution of the number of objects over the considered paths determines which path suffers the minimum attenuation and is hence selected by beamsteering.

We assume that the joint distribution of the number of objects over the available paths is the one resulting from considering as independent the Poisson point processes obtained by restricting the original point process to the region of interest for each path. This is reasonable for the case in which paths do not overlap significantly, and objects are small, otherwise the restriction to one path cannot be regarded as independent from the restriction to another path, because an object could obstruct two or more paths.

For a vector $\mathbf{n}$ of elements $\{n_k\}$, containing the number of objects obstructing the direct link and the primary reflection paths, the joint probability distribution under the above

assumptions is a joint Poisson distribution:

$$\Pr(\mathbf{n}) = e^{-\sum_k N_k} \cdot \prod_k \frac{(N_k)^{n_k}}{n_k!}, \tag{8}$$

where N_k is the average number of obstructions on path k. In practice, this is appropriate for small obstructions covering small fractions of the lengths traveled by the mmwaves, and for negligible probability for one object to obstruct more than one path. The probability to use path i is therefore

$$\begin{aligned}\pi_i &= \sum_{\mathbf{n}=\mathbf{0}}^{\infty} \Pr(\mathbf{n}) \Pr(i = \arg\min_k \{L_k + 10\ \log_{10} \mu_k + z\, n_k\, l_o\}) \\ &= e^{-\sum_k N_k} \sum_{n_i=0}^{\infty} \frac{N_i^{n_i}}{n_i!} \prod_{k \neq i} \sum_{n_k=n_k^{(i)}}^{\infty} \frac{N_k^{n_k}}{n_k!},\end{aligned} \tag{9}$$

where the minimum index in the rightmost sum is the smallest integer number of objects on path k such that the attenuation on path i is smaller than on path k.

With the same approximation, each path attenuation r.v. is described by masses of probability of amplitude equal to the weights of a Poisson distribution, centered at $\mu_k 10^{\frac{L_k + z n_k l_o}{10}}$, $n_k \geq 0$ (in linear units). We can denote by $F_k(\cdot)$ the CDF of the path attenuation r.v.'s, expressed in linear units, and consider such r.v.'s as independent, since we have assumed that the numbers of obstructions on the paths are independent r.v.'s. Therefore, the complementary CDF of Ψ, which is the minimum path attenuation, is the product of the complementary CDF's of the path attenuation r.v.'s, i.e.:

$$1 - F_\Psi(x) = \prod_k \left(1 - e^{-N_k} \sum_{n_k=0}^{\infty} \frac{N_k^{n_k}}{n_k!} u\left(x - \mu_k 10^{\frac{L_k + z n_k l_o}{10}}\right)\right), \tag{10}$$

where $u(\cdot)$ is the unit step function.

We can finally derive the probability density function (pdf) of Ψ, namely $f_\Psi(\cdot)$, by calculating the derivative of $F_\Psi(\cdot)$. By plugging this result into (7), we obtain an approximate formula for the outage probability:

$$\begin{aligned}&P_{\text{out}}(\gamma_{\text{th}}) = \\ &1 - e^{-\sum_k N_k} \sum_i \sum_{n_i=0}^{\infty} \frac{N_i^{n_i}}{n_i!} e^{-B\gamma_{\text{th}}\mu_i 10^{\frac{L_i + z n_i l_o}{10}}} \prod_{k \neq i} \sum_{n_k=n_k^{(i)}}^{\infty} \frac{N_k^{n_k}}{n_k!}.\end{aligned} \tag{11}$$

4.3 Sensitive area with convex-shaped obstructions

In the case of convex objects, which is depicted in Fig. 1 for the direct link, in the special case of a regular pentagon with given rotation ϕ, the maximum per-object obstruction length is $s = h(\phi)$. The center of objects can only be in the rectangle of size $s \times d$, minus the area of the obstruction itself (which accounts for the fact that obstructions cannot overlap the endpoints of a link). Note that $h(\phi)$ is the orthogonal projection of the obstruction shape with respect to the direction of the ray, and its value depends on the rotation angle ϕ. The average over ϕ is given by the Cauchy-Crofton formula as $\bar{h} = P/\pi$, which is a result valid for the orthogonal projection of any 2D line of length P, and hence it holds also for closed curves representing the perimeter of an object rotated uniformly at random. As a consequence, the measure of A_1 for the case of generic convex obstructions of area S and perimeter P is expressed as follows:[1]

$$A_1 = Pd/\pi - S = (d/l_o - 1)\, S. \tag{12}$$

We use the same computation for all paths, using the total length of the path after reflection, and neglecting border effects that slightly reduce the number of obstructions counted next to the reflection point. Hence, our approximation counts more obstructions than needed. However, with small and sparse obstructions, this is not critical, as shown next.

5 NUMERICAL RESULTS

We explore the properties of our model in two representative use cases: one indoor, with possible reflections of the mmwave transmission on the four walls; the other outdoor, with reflections on the buildings at the sides of a street. We numerically evaluate the expressions presented in the previous sections, and compare their predictions to the results of a simulator written in C++ that accounts for randomly placed obstruction lengths, without approximations, and for Rayleigh fading.

5.1 The indoor case

For all results that we present in this case, except when otherwise specified, we consider a room of width 20 m and length 30 m, which is represented as a rectangle over a plane with origin at the lower left corner of the rectangle; using 1 m units, the mmwave transmitter is placed in $[1, 1]$, and the receiver is placed at distance d, in $[d/\sqrt{2} + 1, d/\sqrt{2} + 1]$. Except for plots as a function of d, we will use $d = 10$ m. Except for plots as a function of λ, the intensity of the PPP governing the presence of obstructions is set to $\lambda = 0.5$ m^{-2}. We report results for circular and square obstructions. Except for plots as a function of r, circles have radius 0.1 m, while squares have the same area as circular obstructions. We assume unit fading power (i.e., $\mu = 1$), total antenna gain $G = 30$ dB[2], transmission power $P_{Tx} = 0.1$ W, $\sigma^2 = 1.65 \cdot 10^{-11}$ W, obstruction attenuation z equal to either 80 or 300 dB/m, refractive indices equal to 1 for air and 1.5 for walls, $M = 0.03$ dB/m, $f = 60$ GHz.

[1] The expression $A_1 = \frac{P}{\pi} d - S$ is valid also for non-convex obstructions.
[2] G is obtained by considering a gain of 20 dB at the transmitter and 10 dB at the receiver, as suggested in [2].

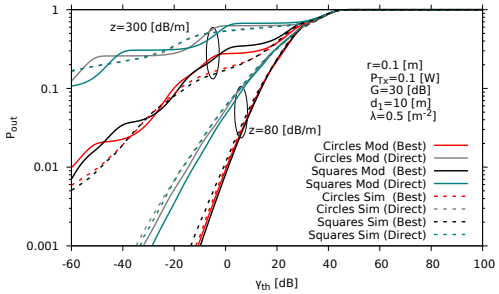

Figure 2: Model and simulation estimates of outage probability in a room of 20 m × 30 m, for circular and square obstructions, for two values of z, for direct and best link selection, versus γ_{th}.

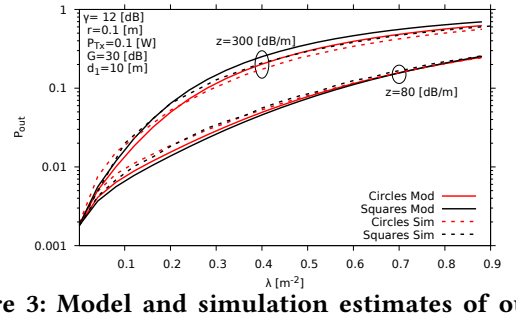

Figure 3: Model and simulation estimates of outage probability in a room of 20 m × 30 m, for circular and square obstructions, for two values of z, versus λ, for best link selection.

Fig. 2 shows the curves of the estimates of P_{out} generated by (11) as well as by simulation. We consider two possibilities for the mmwave link beamsteering. In the first case, the direct path is always selected; in the second case, the path where the attenuation is lowest is selected (this can be the direct path or one of the reflected paths). We can observe from the figure that the model accuracy is very good, especially for lower obstruction attenuation values, in spite of the simplicity and the generality of our proposed approximate model. Obviously, increasing the obstruction attenuation degrades performance by increasing the outage probability for the two obstruction types for both selection cases. Moreover, we see that the impact of beamsteering is quite substantial: the best path selection largely outperforms the direct path selection in terms of outage probability, for a same threshold value. This is an effect of the exploitation of path diversity allowed by beamsteering, thanks to which it is possible to select the path with the least obstruction. Given these observed large performance gains, in the next figures we will focus on the best path selection only.

A special comment is needed to justify the "smoothed staircase" behavior of the curves of P_{out} for the extreme case with $z = 300$ dB/m. This shape is due to the individual contributions of obstructions, each of which corresponds to an exponential term in (11), each progressively shifted by

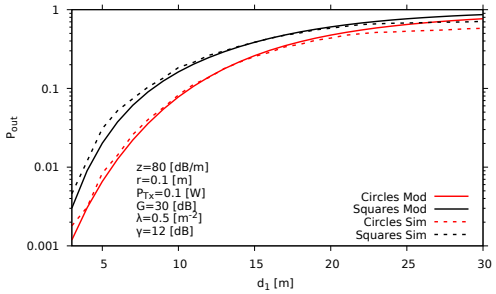

Figure 4: Model and simulation estimates of outage probability in a room of 20 m × 30 m, for circular and square obstructions, for $z = 80$, versus LoS distance, for best link selection.

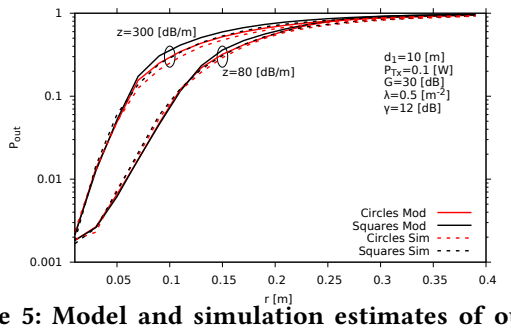

Figure 5: Model and simulation estimates of outage probability in a room of 20 m × 30 m, for circular and square obstructions, for two values of z, versus obstruction size, for the best link selection.

exactly $l_o z$ dB (47 dB for the case of the figure). With the direct path, for values of γ_{th} between -5 and 42 dB, we see the value of P_{out} resulting from the presence of one obstruction (terms with $i = 1$ and $n_i = 0, 1$ in (11)), that in our model is approximated to produce a fixed attenuation $l_o z$. Between -52 and -5 dB, we see the value of P_{out} resulting from the presence of two obstructions (terms with $i = 1$ and $n_i = 0, 1, 2$ in (11)), and so on. As confirmed by observing the curves at $z = 80$, the staircase behaviour is less perceivable with objects that, on average, induce attenuation of the order of a few decibels.

Figs. 3, 4 and 5 report the model and simulation results for the outage probability as a function of three different parameters: obstruction density, link length, and obstruction size, respectively, for the best link selection. The value of γ_{th} is chosen as 12 dB, which provides a reasonable data throughput performance in current standard implementations [1].

From Fig. 3 we see that the increase of the number of obstructions (i.e., of the intensity of the PPP which is used to position obstructions in the room) obviously implies an increase of the outage probability for both values of obstruction attenuation z.

Fig. 4 shows the effect of distance between transmitter and receiver on outage probability. Note that the increase of the

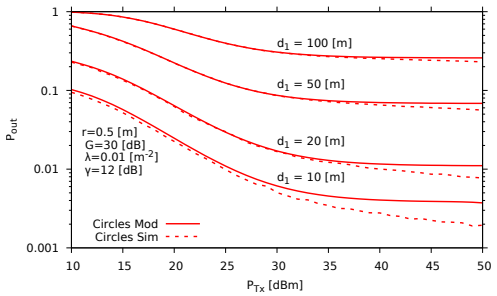

Figure 6: Model and simulation estimates of outage probability in a 100 m long street, for various values of link length, for circular obstructions, with best links selection, versus transmission power.

(primary and reflected) link lengths, in addition to implying higher attenuation, implies a higher number of obstructions that obstruct the link. Both effects lead to an increase of the outage probability at fixed transmission power, as shown in the figure. Note also that in this case we clearly see an impact of the obstruction shape, which was not evident in previous plots.

Finally, Fig. 5 shows plots of the outage probability (model and simulations) for different values of obstruction size. As expected, increases in obstruction size degrade performance.

In all figures, the average number of obstructions is of the order of a few units, less than 4.5 in all cases. The obstruction dimension is chosen so to mimic the presence of human bodies and objects of non-negligible size than can be moved around and obstruct mmwave transmission. In all cases, the values for λ and r are chosen such that $\frac{Nc}{d}$ is less than 3%, i.e., the total obstruction is, on average, a small fraction of the link length. This was chosen in accordance with our model assumption on the low density of obstructions.

5.2 The outdoor case

Fig. 6 shows the outage probability (model and simulations) for circular obstructions in an outdoor environment consisting in a road segment with length 100 m and width 20 m, where Tx is placed at the start of the road, in position [1, 10] m and Rx is placed at a variable distance (10, 20, 50, 100 m) parallel to the horizontal axis of the road. Only reflections on the road sides are considered. The transmission power is varied from 10 mW to 100 W, and circular objects have radius $r = 0.5$ such that the average number of obstructions is of the order of a few units, less than 1.5 in all cases.

We see that the outage probability depends on distance, as expected, and that the model accuracy is very good also in this case, especially in the range of realistic values of P_{Tx}. Shorter distances (10 and 20 m) reach outage probabilities of the order of 1%, but at 10 m distance a transmission power of 25 dBm is sufficient, while 50 dBm are necessary at 20 m. Longer distances are much more problematic.

6 CONCLUSIONS

In this paper we propose a very simple and general approximate model to compute the outage probability in millimeter wave links considering generic obstruction shapes in indoor and outdoor environments. Differently from existing models, we do not consider the presence of an obstruction as a binary variable that causes outage, but we rather account for the cumulative attenuation caused by multiple objects, depending on the obstruction lengths that we characterize stochastically. Also, we explore two cases for path selection: the direct path and the best path selection enabled by the fast beamsteering capability of modern devices. We show that the best path selection largely outperforms the direct path selection in all cases. We prove the usefulness of our model by comparing analytical predictions against simulation results.

ACKNOWLEDGMENTS

The work of V. Mancuso was supported by a Ramon y Cajal grant (ref: RYC-2014-16285) from the Spanish Ministry of Economy and Competitiveness.

REFERENCES

[1] 2012. *IEEE Std 802.11ad-2012* (Dec 2012). https://doi.org/10.1109/IEEESTD.2012.6392842

[2] J G Andrews et al. 2017. Modeling and analyzing millimeter wave cellular systems. *IEEE Trans. Commun.* 65, 1 (2017), 403–430.

[3] T Bai et al. 2014. Analysis of blockage effects on urban cellular networks. *IEEE Trans. Wireless Commun.* 13, 9 (2014), 5070–5083.

[4] T Bai et al. 2014. Analysis of self-body blocking effects in millimeter wave cellular networks. In *Proc. 48th Asilomar Conf.* 1921–1925.

[5] Cisco. 2018. *VNI Global Fixed and Mobile Internet Traffic Forecasts.* https://www.cisco.com/c/en/us/solutions/service-provider/visual-networking-index-vni/index.htm

[6] K Han et al. 2019. Connectivity and Blockage Effects in Millimeter-Wave Air-To-Everything Networks. *IEEE Wireless Commun. Lett.* 8, 2 (2019), 388–391.

[7] I K Jain et al. 2018. Limited by Capacity or Blockage? A Millimeter Wave Blockage Analysis. *arXiv preprint arXiv:1808.01228* (2018).

[8] G R MacCartney et al. 2016. Millimeter-wave human blockage at 73 GHz with a simple double knife-edge diffraction model and extension for directional antennas. In *84th VTC-Fall.* 1–6.

[9] T Nitsche et al. 2014. IEEE 802.11ad: directional 60 GHz communication for multi-Gigabit-per-second Wi-Fi [Invited Paper]. *IEEE Commun. Mag.* 52, 12 (2014), 132–141.

[10] K Rizk et al. 1997. Two-dimensional ray-tracing modeling for propagation prediction in microcellular environments. *IEEE Trans. Veh. Technol.* 46, 2 (1997), 508–518.

[11] J Ryan et al. 2017. Indoor office wideband penetration loss measurements at 73 GHz. In *IEEE Int. Conf. on Commun. Workshops (ICC Workshops).* 228–233.

[12] K Venugopal et al. 2016. Millimeter wave networked wearables in dense indoor environments. *IEEE Access* 4 (2016), 1205–1221.

[13] R J Weiler et al. 2016. Quasi-deterministic millimeter-wave channel models in MiWEBA. *EURASIP Journal on Wireless Commun. and Networking* 2016, 1 (15 Mar 2016), 84. https://doi.org/10.1186/s13638-016-0568-6